Responses to Referee #4's comments

We are grateful to the reviewers for their valuable and helpful comments on our manuscript "Mechanistic Insights into Nitric Sulfuric Acid Formation and Its Enhancement of Sulfuric Acid-Ammonia Nucleation under Severe Urban Pollution" (MS No.: **egusphere-2026-3682**). We have revised the manuscript carefully according to reviewers' comments. The point-to-point responses to the Referee #4's comments are summarized below:

Referee Comments:

The manuscript investigates the formation of nitric sulfuric acid (NSA) from the reaction of SO_3 with HNO_3 and its potential role in sulfuric acid–ammonia nucleation using quantum-chemical calculations and ACDC simulations. The topic is relevant to atmospheric sulfur chemistry and new particle formation, and the attempt to connect molecular formation chemistry with cluster kinetics is potentially useful.

However, after examining the manuscript, I found several substantial inconsistencies in the atmospheric concentration estimates, kinetic comparisons, thermodynamic data, and reported nucleation rates. Some of these affect the physical basis of the main atmospheric conclusions. In particular, the assumed NSA concentrations used in the ACDC calculations are not convincingly connected to the atmospheric conditions discussed in the manuscript.

I therefore recommend Major Revision. A thorough numerical audit and a more conservative interpretation of the atmospheric implications are required before the conclusions can be evaluated reliably.

Response: We would like to thank the reviewer for the positive and valuable comments, and we have revised our manuscript accordingly.

Major issues

Comment 1.

The atmospheric concentration of NSA is not adequately constrained, and the treatment of equilibrium and steady state needs to be corrected.

The manuscript estimates [NSA] from the equilibrium relation, but describes the resulting quantity as a "steady-state concentration." These are not equivalent. A steady-state atmospheric

concentration requires an explicit balance between chemical production and all relevant loss processes. No such loss terms are included here. Are there any NSA atmospheric concentration observations? Why not? Furthermore, the authors should re-examine, and more importantly, the rationale for the coexistence of SO_3 and HNO_3 precursor concentrations in time and space. The authors should therefore re-establish the atmospheric range of [NSA], clearly distinguish equilibrium from steady state, and show how the selected ACDC concentrations are connected to realistic urban tropospheric conditions.

Response: Thank you for this valuable suggestion. The atmospheric concentration range of nitric sulfuric acid (NSA) was reassessed by explicitly accounting for its chemical production and loss processes to obtain a more physically representative estimate of its steady-state concentration. Given the lack of direct quantitative measurements of atmospheric NSA, available observational data for SO_3 and HNO_3 were compiled to constrain the atmospheric conditions under which NSA may form. These observational constraints were subsequently used to define representative atmospheric scenarios for aerosol cluster dynamics code (ACDC) simulations, which were performed to quantify the relative contributions of NSA-containing nucleation pathways under different atmospheric conditions.

(a) To obtain a more representative estimate of atmospheric NSA concentrations, we reassessed its steady-state abundance by accounting for its chemical production and major atmospheric loss processes (Chen et al., 2022). Under steady-state conditions, the production rate of NSA is balanced by its total loss rate, as expressed in Eq. (1):

$$[\mathrm{NSA}] = \frac{k_{\mathrm{R1}}[\mathrm{SO_3}][\mathrm{HNO_3}]}{k_{\mathrm{thermal}} + k_{\mathrm{NSA+OH}}[\mathrm{OH}]} \quad (1)$$

where k_{R1} is the rate coefficient for the SO_3 + HNO_3 reaction, $k_{thermal}$ represents the rate coefficient for the thermal decomposition of NSA (Table S3) and k_{NSA+OH} is the rate coefficient for the reaction of NSA with OH radicals (Long et al., 2022). Here, [SO_3] represents the atmospheric concentration of SO_3, which not only typically ranges from 10^3-10^7 molecules·cm^{-3} but also reach approximately 100 ppb in regions strongly influenced by industrial emissions. [HNO_3] denotes the atmospheric concentration of HNO_3, which generally ranges from 10^8-10^{12} molecules·cm^{-3}. [OH] represents the atmospheric concentration of OH radicals, which was set to 0.75 pptv following Long et al. (2022). It is worth noting that photolytic loss of NSA was not considered in this study,

as its photolytic lifetime is approximately 30 h at 20 km and 12 min at 40 km altitude. These estimates suggest that photolysis is unlikely to represent a major loss pathway for NSA, even under stratospheric conditions. Based on this estimate and considering the concentrations of SO_3 and HNO_3 in heavily polluted environments, an NSA concentration range of 10^3-10^6 molecules·cm^{-3} was adopted in this study for subsequent nucleation simulations. The detailed calculation procedure of the atmospheric concentration of NSA is provided in Part S1 of the Supplement. Based on this, the sentence of "In the absence of atmospheric field measurements for gas-phase NSA, thermodynamic equilibrium calculations were applied to estimate its atmospheric concentration and to assess its potential impact on NPF. The concentration of its key precursor, SO_3, exhibits pronounced regional variability. SO_3 concentrations in regions such as Beijing, are around 10^6 molecules·cm^{-3} (Yao et al., 2020), while substantially higher levels, are observed in in industrial emission zones. Atmospheric NA concentration can similarly approach 10^{12} molecules·cm^{-3}. By combining the plausible concentration ranges of both precursors within the anthropogenically influenced troposphere (258.15-298.15 K), the atmospheric concentration of NSA is estimated to range from 10^3 to 10^7 molecules·cm^{-3}. The detailed calculation of the calculation procedure can be found in Part S1 of the Supplement." has been changed as "In the absence of atmospheric field measurements for gas-phase NSA, the steady-state approximation calculations were applied to estimate its atmospheric concentration and to assess its potential impact on NPF. The corresponding estimation equation is given in Eq. (7).

$$[\mathrm{NSA}] = \frac{k_{\mathrm{R1}}[\mathrm{SO_3}][\mathrm{HNO_3}]}{k_{\mathrm{thermal}} + k_{\mathrm{NSA+OH}}[\mathrm{OH}]} \quad (7)$$

where k_{R1} is the rate coefficient for the SO_3 + HNO_3 reaction, $k_{thermal}$ represents the rate coefficient for the thermal decomposition of NSA (Table S3) and k_{NSA+OH} is the rate coefficient for the reaction of NSA with OH radicals (Long et al., 2022). Here, [SO_3] represents the atmospheric concentration of SO_3, which typically ranges from 10^3-10^7 molecules·cm^{-3}, with reported observations from regions such as Beijing (Yao et al., 2020), Leipzig, the Antarctic Peninsula, and Mace Head (Kumar et al., 2024). Concentrations approaching 100 ppb have also been reported in regions strongly influenced by industrial emissions. [HNO_3] denotes the atmospheric concentration of HNO_3, with reported values spanning 10^8-10^{12} molecules·cm^{-3} across various locations, including Mace Head (Ireland), Melpitz (Germany) (Acker et al., 2010), Beijing

(Li et al., 2024b) and the North China Plain (Xu et al., 2016). [OH] represents the atmospheric concentration of OH radicals, which was set to 0.75 pptv following Long et al. (2022). It is worth noting that photolytic loss of NSA was not considered in this study, as its photolytic lifetime is approximately 30 h at 20 km and 12 min at 40 km altitude (Long et al., (2022). These estimates suggest that photolysis is unlikely to represent a major loss pathway for NSA, even under stratospheric conditions. The steady-state concentration of NSA was estimated to range from 10^3 to 10^6 molecules·cm^{-3} based on reported observations of SO_3 and HNO_3 in regions where both species coexist. The detailed calculation procedure of the atmospheric concentration of NSA is provided in Part S1 of the Supplement." in Lines 187-197 Page 8 to Lines 198-208 Page 9 of the revised manuscript.

Table S3. Parameters for NSA concentration estimation.

T (K)	k_{R1} (cm^3·molecule^{-1}·s^{-1})	$k_{thermal}$ (s^{-1})	k_{NSA+OH} (cm^3·molecule^{-1}·s^{-1})
280	1.42×10^{-13}	454629	6.70×10^{-4}
290	1.16×10^{-13}	712193	
298	9.94×10^{-14}	991601	
300	9.58×10^{-14}	1073180	
310	8.06×10^{-14}	1119480	
320	6.87×10^{-14}	2197540	
275.15	2.46×10^{-13}	333738	
268.65	2.39×10^{-13}	231988	
262.15	2.51×10^{-13}	158407	
255.65	2.64×10^{-13}	106133	

T represents temperature; k_{R1} represents the bimolecular rate coefficient for the SO_3 + HNO_3 reaction; $k_{thermal}$ represents the first-order rate coefficient for the thermal decomposition of NSA; and k_{NSA+OH} represents the bimolecular rate coefficient for the reaction of NSA with OH radicals.

(b) We conducted an extensive literature review but found no direct quantitative measurements of gas-phase NSA concentrations in the atmosphere. Nevertheless, previous atmospheric mass spectrometric studies have detected the $NO_3SO_3^-$ ion (Reiner and Arnold, 1997; Schlager and Arnold, 1987), providing indirect evidence for the presence of NSA-related species in the atmosphere. In the absence of direct observational data, we used the estimated steady-state concentrations of NSA, derived by accounting for its chemical production and loss processes, to further evaluate its potential contribution to new particle formation (NPF) under different

atmospheric conditions.

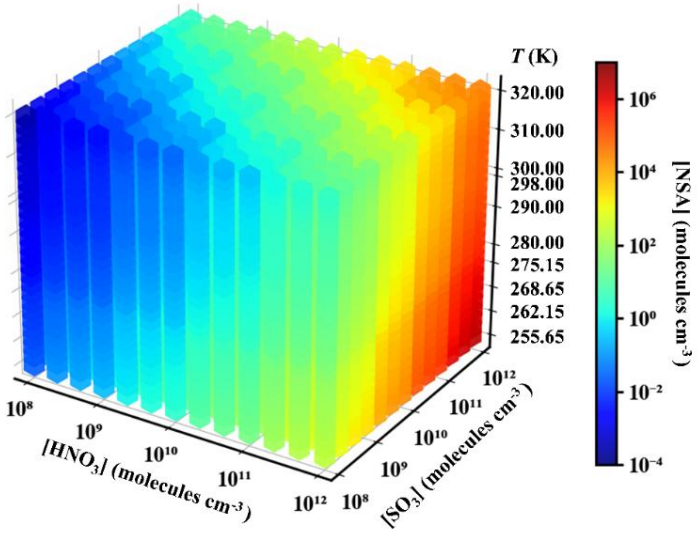


Fig. S3. Estimated steady-state concentrations of NSA as a function of [SO_3], [HNO_3], and temperature under tropospheric conditions. The color scale represents the NSA concentration in molecules·cm^{-3}.

(c) Due to the estimation of the steady-state concentration of NSA depends strongly on the atmospheric concentrations of HNO_3 and SO_3, the reported levels of these precursors are discussed below. (*i*) Atmospheric HNO_3 concentrations vary substantially across regions. Concentrations typically range from approximately 10^8-10^9 molecules·cm^{-3} at Mace Head, Ireland, and Melpitz, Germany (Acker et al., 2010). In polluted urban regions, such as Beijing (Li et al., 2024b) and several sites in South Korea (Jung et al., 2026), concentrations can reach approximately 10^{10} molecules·cm^{-3}. In more heavily polluted regions, including the North China Plain and Qingdao, China, HNO_3 concentrations can increase to approximately 10^{11}-10^{12} molecules·cm^{-3}. Accordingly, this study adopted a concentration range of 10^8-10^{12} molecules·cm^{-3} to encompass the reported levels across different atmospheric environments. (*ii*) Field observations have confirmed the presence of gaseous SO_3 across a wide range of atmospheric environments. Concentrations of 10^3-10^4 molecules·cm^{-3} have been reported in Beijing during summer (Acker et al., 2010), whereas levels of 10^4-10^5 molecules·cm^{-3} have been observed in Beijing, Leipzig (Kumar et al., 2024), the Antarctic Peninsula and Maido. Higher concentrations of 10^5-10^6 molecules·cm^{-3} have been reported in Beijing during winter, while levels approaching 10^7 molecules·cm^{-3} have occasionally been recorded at Mace Head. In addition, SO_3 concentrations of approximately 100 ppb were reported in regions strongly influenced by industrial emissions (Sarbassov et al., 2018). Overall, these observations demonstrate the

widespread occurrence of atmospheric SO_3 and HNO_3 and their pronounced spatial variability.

Atmospheric SO_3 and HNO_3 have both been detected in various atmospheric environments, suggesting the potential for their coexistence and subsequent NSA formation. For example, in Beijing, SO_3 concentrations range from approximately 5.0×10^3 - 1.9×10^6 molecules·cm^{-3}, while HNO_3 concentrations average approximately 3.0×10^{10} molecules·cm^{-3}. At Mace Head, Ireland, SO_3 concentrations can reach approximately 10^7 molecules·cm^{-3}, while HNO_3 concentrations range from 4.8×10^8 to 2.9×10^9 molecules·cm^{-3}. The reported occurrence of both precursors in Beijing and at Mace Head suggests that NSA may potentially form in urban and coastal marine environments. Based on the above analysis, the sentence of "[SA] fluctuated between 10^4 to 10^8 molecules·cm^{-3} (Rong et al., 2020; Almeida et al., 2013; Kuang et al., 2008), while [A] ranged from 10^7 to 10^{11} molecules·cm^{-3} (Liu et al., 2021) and the corresponding [NSA] was between 10^3 and 10^7 molecules·cm^{-3}." has been changed as "[SA] fluctuated between 10^4 to 10^8 molecules·cm^{-3} (Rong et al., 2020; Almeida et al., 2013; Kuang et al., 2008), while [A] ranged from 10^7 to 10^{11} molecules·cm^{-3} (Liu et al., 2021). In the absence of direct atmospheric measurements of gas-phase NSA, a concentration range of 10^3-10^6 molecules·cm^{-3} was selected based on reported SO_3 and HNO_3 concentrations under heavily polluted conditions." in Line 130-134 Page 6 of the revised manuscript.

(d) The concentrations of the gaseous precursors H_2SO_4 and NH_3 used in the ACDC simulation in this study were primarily derived from field observations (Beck et al., 2022; Berresheim et al., 2002; Wentworth et al., 2016; Yao and Zhang, 2016; Nair and Yu, 2020). Furthermore, the steady-state concentration of NSA was estimated to range from 10^3 to 10^6 molecules·cm^{-3} based on reported observations of SO_3 and HNO_3 in regions where both species coexist. These estimates were then incorporated into ACDC simulations to systematically assess the role of NSA in SA-A nucleation. The corresponding results are presented in Fig. 6. The simulations indicate that NSA-mediated nucleation pathways can contribute substantially to new particle formation under conditions of low [SA] and high [NSA] and [A], consistent with those in regions such as Beijing and Mace Head, Ireland, where relatively high concentrations of SO_3 and HNO_3 have been reported.

Reference:

Acker, K., Wieprecht, W., and Möller, D.: Multiphase studies in continental and marine

atmospheres, http://meetings.copernicus.org/fog2010, 2010.

Beck, L. J., Schobesberger, S., Sipilä, M., Kerminen, V. M., and Kulmala, M.: Estimation of sulfuric acid concentration using ambient ion composition and concentration data obtained with atmospheric pressure interface time-of-flight ion mass spectrometer, Atmos. Meas. Tech., 15, 1957-1965, https://doi.org/10.5194/amt-15-1957-2022, 2022.

Berresheim, H., Elste T., Tremmel, H. G., Allen, A. G., Hansson, H. C., Rosman, K., Dal Maso, M., Mäkelä, J. M., Kulmala, M., and O'Dowd, C. D.: Gas-aerosol relationships of H_2SO_4, MSA, and OH: Observations in the coastal marine boundary layer at Mace Head, Ireland, J. Geophys. Res., 107, 8100, https://doi.org/10.1029/2000JD000229, 2002.

Chen, X., Wang, H., and Lu, K.: Interpretation of NO_3-N_2O_5 observation via steady state in high-aerosol air mass: the impact of equilibrium coefficient in ambient conditions, Atmos. Chem. Phys., 22, 3525-3533, https://doi.org/10.5194/acp-22-3525-2022, 2022.

Jung, D., Song, J., Kim, K., Kang, S., Kim, Y., Hong, S.-C., Lee, J.-B., Seo, S.-J., Lee, K., Park, J.-S., Song, M., Choi, N. R., and Lee, T.: Spatial and Seasonal Variation of Nitric Acid (HNO_3) and Understanding the Formation of NH_4NO_3 in the HNO_3-NH_3 system in Korea, Aerosol Air Qual. Res., 26, 19, https://doi.org/10.1007/s44408-025-00090-2, 2026.

Kumar, A., Iyer, S., Barua, S., Brean, J., Besic, E., Seal, P., Dall'Osto, M., Beddows, D. C. S., Sarnela, N., Jokinen, T., Sipilä, M., Harrison, R. M., and Rissanen, M.: Direct measurements of covalently bonded sulfuric anhydrides from gas-phase reactions of SO_3 with acids under ambient conditions, J. Am. Chem. Soc., 146, 15562-15575, https://doi.org/10.1021/jacs.4c04531, 2024.

Li, Y., Li, X., Cai, R., Yan, C., Zheng, G., Li, Y., Chen, Y., Zhang, Y., Guo, Y., Hua, C., Kerminen, V.-M., Liu, Y., Kulmala, M., Hao, J., Smith, J. N., and Jiang, J.: The significant role of new particle composition and morphology on the HNO_3-driven growth of particles down to Sub-10 nm, Environ. Sci. Technol., 58, 5442-5452, https://doi.org/10.1021/acs.est.3c09454, 2024b.

Long, B., Xia, Y., Bao, J. L., Carmona-García, J., Gómez Martín, J. C., Plane, J. M. C., Saiz-Lopez, A., Roca-Sanjuán, D., and Francisco, J. S.: Reaction of SO_3 with $HONO_2$ and implications for sulfur partitioning in the atmosphere, J. Am. Chem. Soc., 144, 9172-9177, https://doi.org/10.1021/jacs.2c03499, 2022.

Nair, A. A., and Yu, F.: Quantification of atmospheric ammonia concentrations: A review of its measurement and modeling, Atmosphere, 11, 1092, https://doi.org/10.3390/atmos11101092, 2020.

Reiner, T., and Arnold, F.: Stratospheric SO_3: Upper limits inferred from ion composition measurements-Implications for H_2SO_4 and aerosol formation, 24, 1751-1754, https://doi.org/10.1029/97GL01758, 1997.

Sarbassov, Y., Duan, L., Manovic, V., and Anthony, E. J.: Sulfur trioxide formation/emissions in coal-fired air- and oxy-fuel combustion processes: a review, Greenhouse Gas. Sci. Technol., 8, 402-428, https://doi.org/10.1002/ghg.1767, 2018.

Schlager, H., and Arnold, F.: Balloon-borne composition measurements of stratospheric negative ions and inferred sulfuric acid vapor abundances during the MAP/GLOBUS 1983 campaign, Planet. Space Sci., 35, 693-701, https://doi.org/10.1016/0032-0633(87)90136-X, 1987.

Wentworth, G. R., Murphy, J. G., Croft, B., Martin, R. V., Pierce, J. R., Côté, J. S., Courchesne, I., Tremblay, J. É., Gagnon, J., Thomas, J. L., Sharma, S., Toom-Sauntry, D., Chivulescu, A., Levasseur, M., and Abbatt, J. P. D.: Ammonia in the summertime Arctic marine boundary layer: sources, sinks, and implications, Atmos. Chem. Phys., 16, 1937-1953, https://doi.org/10.5194/acp-

16-1937-2016, 2016.
Xu, W., Wu, Q., Liu, X., Tang, A., Dore, A. J., and Heal, M. R.: Characteristics of ammonia, acid gases, and $PM_{2.5}$ for three typical land-use types in the North China Plain, Environ. Sci. Pollut. Res., 23, 1158-1172, https://doi.org/10.1007/s11356-015-5648-3, 2016.
Yao, L., Fan, X., Yan, C., Kurtén, T., Daellenbach, K. R., Li, C., Wang, Y., Guo, Y., Dada, L., Rissanen, M. P., Cai, J., Tham, Y. J., Zha, Q., Zhang, S., Du, W., Yu, M., Zheng, F., Zhou, Y., Kontkanen, J., Chan, T., Shen, J., Kujansuu, J. T., Kangasluoma, J., Jiang, J., Wang, L., Worsnop, D. R., Petäjä, T., Kerminen, V.-M., Liu, Y., Chu, B., He, H., Kulmala, M., and Bianchi, F.: Unprecedented Ambient Sulfur Trioxide (SO_3) Detection: Possible Formation Mechanism and Atmospheric Implications, Environ. Sci. Technol. Lett., 7, 809-818, https://doi.org/10.1021/acs.estlett.0c00615, 2020.
Yao, X., and Zhang, L.: Trends in atmospheric ammonia at urban, rural, and remote sites across North America, Atmos. Chem. Phys., 16, 11465-11475, https://doi.org/10.5194/acp-16-11465-2016, 2016.

Comment 2.

The chemical classification of NSA should be reconsidered.

The manuscript introduces nitric sulfuric acid (NSA, O_2NOSO_3H) within the context of organosulfates and later refers to the present results as providing insight into the role of OSs in aerosol nucleation. However, the NSA species studied here contains no carbon and therefore should not be classified as an organosulfate in the conventional sense. This is not merely a terminology issue, because the current Introduction and Conclusion use the organosulfate framework to motivate and interpret the study. The authors should revise this part of the manuscript, clearly distinguish NSA from true organosulfates such as methyl hydrogen sulfate and glycolic acid sulfate, and use a chemically appropriate description for NSA throughout.

Response: Thank you for this valuable suggestion. We sincerely apologize for the incorrect classification of NSA in the original manuscript. In response to the reviewer's comment, we have revised the relevant descriptions of NSA throughout the manuscript, including the Abstract and Conclusions. We agree with the reviewer that NSA (O_2NOSO_3H) should not be classified as an organosulfate (OS), as its molecular structure contains no carbon atom.

To address this issue, we have revised the Introduction to remove the inappropriate association of NSA with organosulfates and to establish a more chemically appropriate context for the present study. Specifically, the sentence of "Organosulfates (OSs) constitute an important component of secondary organic aerosols (SOA). Although previous studies have investigated the

aerosol nucleation of OSs such as glycolic acid sulfate and methyl hydrogen sulfate, exploring the aerosol nucleation behavior of additional OSs remains essential." has been changed as "The reaction products of SO_3 with important atmospheric trace species, such as NH_3, H_2SO_4, and methanol, and their impacts on new particle formation (NPF) have been extensively investigated. However, the influence of O_2NOSO_3H (NSA), formed from the reaction between SO_3 and HNO_3, on NPF remains largely unexplored, limiting a comprehensive assessment of the potential contribution of SO_3 and HNO_3 chemistry to NPF under highly polluted atmospheric conditions." in Lines 11-15 Page 1 of the revised manuscript. Meanwhile, the sentence of "This study not only deepens the understanding of the gas-phase formation mechanisms of NSA but also provides new insights into the roles of OSs in aerosol nucleation under heavily polluted urban conditions." has been changed as "This study not only deepens the understanding of the gas-phase formation mechanisms of NSA but also provides new insights into the roles of NSA in aerosol nucleation under heavily polluted urban conditions." in Lines 439-441 Page 19 of the revised manuscript.

Overall, the organosulfate examples cited in the Introduction were intended to illustrate the reactivity of SO_3 toward trace atmospheric species, rather than to classify NSA as an organosulfate. Specifically, the formation of methyl hydrogen sulfate and glycolic acid sulfate motivated us to investigate whether SO_3 could similarly react with HNO_3 to form the carbon-free species NSA.

Comment 3.

The thermodynamic data do not support the general statement that NSA incorporation systematically stabilizes the clusters.

The manuscript repeatedly states that increasing NSA content lowers the formation free energy and systematically stabilizes SA-A clusters. However, Table S7 shows clear counterexamples. At 278.15 K, for example, the formation free energies of $(SA)_2 \cdot A$, $SA \cdot A \cdot NSA$, and $A \cdot (NSA)_2$ are approximately -22.03, -21.66, and -20.46 $kcal \cdot mol^{-1}$, respectively. Thus, replacing SA with NSA in this composition makes the formation free energy less negative rather than more negative.

Response: Thank you for this valuable suggestion. We agree that the Gibbs free energy of formation (ΔG) does not decrease systematically upon the addition of NSA for clusters containing the same total number of acid and base molecules. The corresponding major revision has been

made as follows.

(a) To facilitate a clearer understanding of the thermodynamic results and avoid potential misinterpretation, Fig. 3 has been replotted in the revised manuscript to ensure consistency between the graphical presentation and our interpretation of the thermodynamic data.

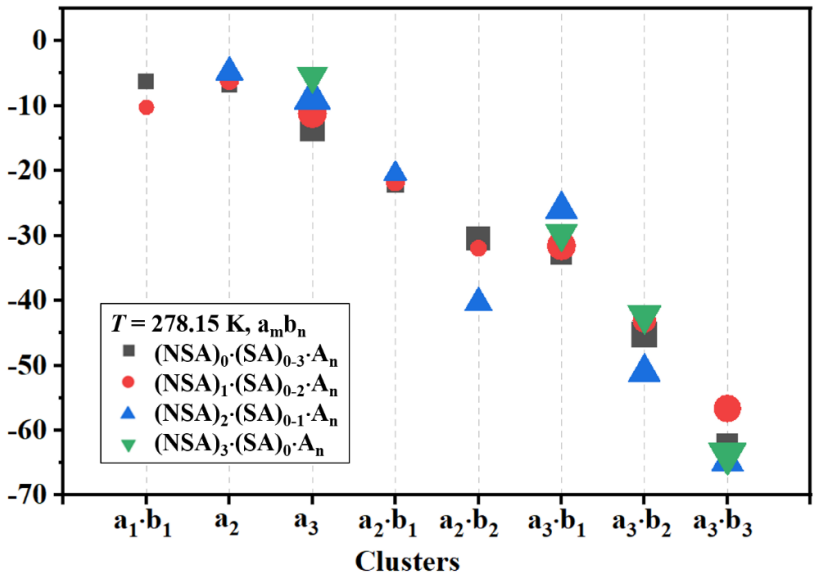


Fig. 3 Gibbs formation free energies (ΔG, kcal·mol^{-1}) of $a_m b_n$ clusters (a = acid ($(NSA)_x(SA)_y$), b = base (A), $0 \le n \le m \le 3$, $0 \le x \le m$, $0 \le y \le m$, and $x + y = m$ at 278.15 K at the DLPNO-CCSD(T)/aug-cc-pVTZ//M06-2X/6-311++G(2*df*,2*pd*) level of theory; The circles of different sizes indicate the sizes of the corresponding clusters.

(b) Similar comparative approaches have been adopted in previous studies (***Atmos. Chem. Phys.***, 2026, 26, 3091-3105; ***Atmos. Chem. Phys.***, 2026, 26, 3867-3880; ***Atmos. Environ.***, 2018, 189, 244-251; ***Phys. Chem. Chem. Phys.***, 2018, 20, 17406-17414). Following these studies, we focus on comparing ternary SA-A-NSA clusters with their corresponding binary SA-A clusters to evaluate the effect of NSA incorporation on thermodynamic stability.

(c) We agree that the Gibbs free energy of formation (ΔG) does not decrease systematically with increasing NSA content for clusters containing the same total number of acid and base molecules. Our primary objective was to investigate how the incorporation of an NSA molecule affects the thermodynamic stability of the corresponding SA-A clusters, rather than to distinguish the competitive effects between NSA and SA. Accordingly, we focused on pairwise comparisons between clusters with and without NSA, specifically SA·A·NSA versus SA·A and $(SA)_2$·A·NSA versus $(SA)_2$·A. To avoid potential confusion, the sentence of "For clusters containing the same total number of acid and base molecules, ΔG decreases systematically with increasing numbers of NSA molecules, indicating NSA incorporation progressively enhances thermodynamic stability."

has been changed as "Ternary SA-A-NSA clusters consistently demonstrated lower ΔG values compared to their binary counterparts. For example, the ΔG of SA·A·NSA and $(SA)_2$·A·NSA are 15.41 and 9.53 kcal·mol^{-1} lower, respectively, than those of SA·A and $(SA)_2$·A, indicating that NSA can enhance the thermodynamic stability of SA-A clusters." in Lines 249-252 Page 11 of the revised manuscript.

Comment 4.

The enhancement-factor analysis in Fig. 8 is currently not reproducible from the information provided.

The manuscript defines the NSA enhancement factor as the ratio between the cluster formation rates with and without NSA. However, how to get the values reported in Fig. 8? > 10^{10}? In addition, the Fig. 8 caption refers to 238.15 K, any reported ACDC calculations?

The manuscript draws a strong quantitative conclusion that NSA enhances nucleation by many orders of magnitude more than NA, yet the corresponding NA thermodynamic data, evaporation rates, and ACDC results are not provided in sufficient detail for independent verification. The authors should provide the complete underlying data and clarify the temperature and calculation conditions used for Fig. 8.

Response: Thank you for this valuable suggestion. We apologize for the insufficient information provided in the original manuscript regarding the enhancement-factor analysis in Fig. 8. According to the reviewer's suggestion, the corresponding ACDC simulation results for the SA-A-NSA system at 238.15 K have been provided in Table S17 of the revised Supporting Information. The thermodynamic data, evaporation rates, and ACDC simulation results for the SA-A-NA system were obtained from a previous study (***Phys. Chem. Chem. Phys.***, 2018, 20, 17406-17414). The corresponding major revision has been made as follows.

(a) We acknowledge that the original manuscript did not provide sufficient information to fully explain the enhancement-factor analysis presented in Fig. 7. To provide a clearer presentation of the results, the corresponding ACDC simulation results for the SA-A-NSA system at 238.15 K have been provided in Table S17 of the revised Supporting Information.

(b) The thermodynamic data, evaporation rates, and ACDC simulation results for SA-A-NA system used in the comparison were obtained from previously published work (***Phys. Chem.***

Chem. Phys., 2018, 20, 17406-17414). These published data were used as the basis for comparison with the corresponding NSA results, allowing the enhancement effect associated with NSA to be evaluated relative to the NA system. Based on this, the sentence of "The thermodynamic data and total evaporation rates for the SA-A-NA system were obtained from a previous study (Liu et al., 2018)." has been added in Lines 374-375 Page 16 of the revised manuscript.

Table S17. Nucleation rate $J_{SA\text{-}A\text{-}NSA}$ and enhancement factor R for the SA-A-NSA system at 238.15 K as a function of NSA monomer concentration (units: molecules·cm^{-3}).

[NSA] (molecules·cm^{-3})	10^0	10^3	10^4	10^5	10^6	10^7
$J_{SA\text{-}A\text{-}NSA}$	1.81E-16	2.30E-14	4.02E-11	2.37E-07	2.10E-05	1.34E-03
R		1.27E+02	2.22E+05	1.31E+09	1.16E+11	7.39E+12

Comment 5.

The atmospheric interpretation is too broad relative to the actual simulation design.

The manuscript repeatedly associates individual simulation conditions with specific environments such as Beijing, Hyytiälä, the Arctic, or polluted urban regions. However, the input parameters are assembled from different literature sources rather than representing simultaneous, site-specific observations. The SI also invokes stratospheric and geoengineering scenarios to justify very high SO_3 concentrations, while the main manuscript interprets the resulting NSA concentrations primarily in the context of urban tropospheric pollution. These are distinct atmospheric environments and should not be conflated. The authors should either provide genuinely site-specific input combinations or describe the calculations as idealized sensitivity scenarios. Statements such as a given pathway contributing a certain percentage "at Hyytiälä" or "in the Arctic" should be avoided unless the complete set of model inputs is representative of those environments.

Response: Thank you for this valuable suggestion. We apologize for repeatedly linking specific simulation conditions to environments such as Beijing, Hyytiälä, the Arctic, and polluted urban areas in the original manuscript. We agree that the input concentrations collected from different literature sources do not necessarily represent simultaneous observations at the same location. The main purpose of the ACDC simulations is to investigate how NSA affects SA-A nucleation and

how changes in temperature and precursor concentrations influence the relative contributions of different nucleation pathways. Therefore, these simulations are intended to explore the effects of varying atmospheric conditions based on reported concentration ranges, rather than to directly represent nucleation processes at specific locations. Furthermore, to provide a more comprehensive assessment of the effects of varying atmospheric conditions, we have replotted the three-dimensional distribution in Fig. 5(c) to systematically examine the combined influence of NSA, SA, and A concentrations on the relative contributions of different cluster growth pathways.

(a) The H_2SO_4 and NH_3 concentrations used in the ACDC simulations were selected based on atmospheric concentration ranges reported in the literature (Beck et al., 2022; Berresheim et al., 2002; Wentworth et al., 2016; Yao and Zhang, 2016; Nair and Yu, 2020). In contrast, the NSA concentrations were determined from the production and loss processes considered in this study to estimate its steady-state concentration range. Although the input parameters were compiled from different literature sources and do not necessarily represent simultaneous observations at the same location, in analyzing the influence of sulfuric acid (SA) concentration on the contributions of different cluster growth pathways, the SA concentrations used were derived from observational data reported in the literature for the corresponding regions. By using these site-specific observed concentrations, we further evaluated how variations in SA concentration under different atmospheric conditions affect the relative contributions of different nucleation pathways.

(b) Field observations have confirmed the presence of gaseous SO_3 across a wide range of atmospheric environments. Concentrations of 10^3-10^4 molecules·cm^{-3} have been reported in Beijing during summer, whereas levels of 10^4-10^5 molecules·cm^{-3} have been observed in Beijing (Yao et al., 2020), Leipzig, the Antarctic Peninsula, Mace Head (Kumar et al., 2024). Higher concentrations of 10^5-10^6 molecules·cm^{-3} have been reported in Beijing during winter, while levels approaching 10^7 molecules·cm^{-3} have occasionally been recorded at Mace Head (Kumar et al., 2024). In addition, SO_3 concentrations of approximately 100 ppb were reported in regions strongly influenced by industrial emissions (Sarbassov et al., 2018). We acknowledge that the high SO_3 concentrations discussed in the context of stratospheric observations and geoengineering scenarios pertain to atmospheric conditions distinct from those of the urban troposphere. Accordingly, the simulations involving these elevated SO_3 concentrations are interpreted as idealized sensitivity scenarios intended to explore the potential influence of SO_3 availability on

NSA formation and the associated nucleation pathways, rather than as direct representations of urban tropospheric conditions.

(c) Following the reviewer's suggestion, we have replotted the three-dimensional distribution of the combined effects of [NSA], [SA], and [A] on the contributions of cluster growth pathways, as shown in revised Fig. 5(c). This plot simultaneously considers variations in the concentrations of all three precursors and provides a more comprehensive representation of the variation characteristics of cluster growth pathway contributions under their combined effects. Based on the above analysis, the sentence of "The relative contributions of NSA-involved and non-NSA pathways to cluster growth are quantitatively evaluated using the flux-out branching ratio under different conditions. As shown in Fig. 6(b), at 278.15 K with [SA] = 10^6 molecules·cm^{-3} and [A] = 10^9 molecules·cm^{-3}, the nucleation mechanism exhibits a strong dependence on [NSA]. At low NSA concentrations (10^3-10^4 molecules·cm^{-3}), representative of conditions such as southern Ontario, Canada (Zbieranowski and Aherne, 2012), cluster growth proceeds almost exclusively via the non-NSA pathway. As [NSA] increases to 10^5 molecules·cm^{-3} (e.g., Korea) (Jung et al., 2026), the NSA-involved pathway begins to emerge but still contributes only marginally to the overall flux. When [NSA] further increases to 10^6-10^7 molecules·cm^{-3}, as in the North China Plain (Nair and Yu, 2020), the NSA-involved pathway rapidly becomes dominant, with its contribution approaching unity, indicating that NSA can substantially enhance nucleation in the SA-A-NSA system. In contrast, at [NSA] = 10^6 molecules·cm^{-3}, *T* exerts a relatively minor influence on pathway partitioning (Fig. 6(c)). Over the *T* range of 258.15-298.15 K, a slight increase in T marginally enhances the contribution of the non-NSA pathway; however, the NSA-involved pathway remains dominant throughout, consistently accounting for more than 80% of the total flux. These results further confirm that NSA plays a decisive role in steering the cluster growth mechanism under atmospherically relevant conditions.

As shown in Fig. 6(d), the contribution of NSA to SA-A aerosol nucleation increases markedly with decreasing [SA]. Under low-SA conditions (10^4 molecules·cm^{-3}), such as those observed in Hyytiälä (Beck et al., 2022), the NSA-involved pathway dominates cluster formation, contributing approximately 98% of the total nucleation flux. As [SA] increases to 10^6 molecules·cm^{-3} (e.g., the western coast of Ireland (Berresheim et al., 2002)), the contribution of the SA-A-NSA pathway decreases slightly to 95%. However, at higher SA levels (10^7

molecules·cm^{-3}), the NSA-involved pathway is strongly suppressed, accounting for only 3% of the total flux, indicating that low [SA] are more favorable for SA-A-NSA nucleation.

In addition, the contribution of the SA-A-NSA pathway is negatively correlated with [A], as illustrated in Fig. 6(e). In regions with low [A] (10^8 molecules·cm^{-3}), such as Baffin Bay and the eastern Canadian Arctic Archipelago (40-870 pptv) (Wentworth et al., 2016), the NSA-involved pathway contributes about 95%, while the binary SA-A nucleation is nearly negligible. As [A] increases to an intermediate level, typical of Canada (0.8-2.6 ppbv) and America (1.6-4.9 ppbv) (Yao and Zhang, 2016), the contribution of the NSA-involved pathway decreases slightly from 95% to 92%. At even higher [A] (10^{11} molecules·cm^{-3}), such as those observed in Midwest US and the North China Plain (20-74 ppbv) (Nair and Yu, 2020), its contribution is further reduced to 88%, although it remains the dominant nucleation route." has been changed as "The relative contributions of NSA-involved pathways to cluster growth are quantitatively evaluated using the flux-out branching ratio under different conditions. As shown in Fig. 5(b), at [NSA] = 10^6 molecules·cm^{-3}, *T* exerts a relatively minor influence on pathway partitioning (Fig. 5(c)). Over the *T* range of 258.15-298.15 K, a slight increase in *T* marginally enhances the contribution of the SA-A pathway; however, the NSA-involved pathway remains dominant throughout, consistently accounting for more than 80% of the total flux. These results further confirm that NSA plays a decisive role in steering the cluster growth mechanism under atmospherically relevant conditions.

Fig. 5(c) shows the combined effects of the concentrations of the aerosol precursors on the contribution of the SA-A-NSA pathway to cluster growth. Overall, the contribution of the SA-A-NSA pathway to cluster growth exhibits a strong dependence on [NSA] and [SA], while showing comparatively weaker sensitivity to variations in [A]. At [NSA] = 10^3 molecules·cm^{-3} and [SA] = 10^4 molecules·cm^{-3}, the SA-A-NSA pathway contributes negligibly at [A] < 10^{11} molecules·cm^{-3}, consistent with the low A levels reported in Baffin Bay, the eastern Canadian Arctic Archipelago (Wentworth et al., 2016) and America (Yao and Zhang, 2016). Its contribution reaches 45% only at [A] = 10^{11} molecules·cm^{-3}. By contrast, at [NSA] = 10^4 molecules·cm^{-3} and [SA] = 10^4 molecules·cm^{-3}, the contribution of the SA-A-NSA pathway decreases only slightly from 95% to 89% as [A] increases from 10^7 to 10^{11} molecules·cm^{-3}. However, when [SA] increases to 10^5 molecules·cm^{-3}, the contribution of the SA-A-NSA pathway drops to nearly zero at [A] < 10^{11} molecules·cm^{-3}, as reported in Midwest and the North China Plain (Nair and Yu, 2020), but rises

to approximately 45% at [A] = 10^{11} molecules·cm^{-3}. These results indicate that under low [NSA] conditions, the SA-A-NSA pathway contributes substantially primarily at low [SA], while showing high sensitivity to increases in [SA].

As [NSA] increases to 10^5 molecules·cm^{-3}, the contribution of the SA-A-NSA pathway increases substantially, reaching 89%-99% at [SA] ≤ 10^5 molecules·cm^{-3}, consistent with the low SA concentrations reported in Hyytiälä (Beck et al., 2022), and remains relatively insensitive to [A] variations across the range of 10^7-10^{11} molecules·cm^{-3}. At higher [NSA] levels (10^6 molecules·cm^{-3}), the contribution of the SA-A-NSA pathway remains generally comparable to that at [NSA] = 10^5 molecules·cm^{-3}, suggesting that its contribution tends to level off with further increases in [NSA]. Under low [SA] conditions (10^4-10^6 molecules·cm^{-3}), consistent with the lower concentrations reported in Hyytiälä (Beck et al., 2022) and along the west coast of Ireland (Berresheim et al., 2002), and high [A] (10^{11} molecules·cm^{-3}), comparable to those observed in the Midwestern United States and the North China Plain (Nair and Yu, 2020), the contribution of the SA-A-NSA pathway remains within 88%-99%. However, when [SA] increases to 10^8 molecules·cm^{-3}, its contribution approaches zero regardless of [NSA] and [A], indicating that the contribution of the binary SA-A nucleation pathway increases substantially under high [SA] conditions, thereby reducing the relative contribution of the SA-A-NSA pathway." has been added in Lines 304-309 Page 13 to Lines 310-311 Page 14 of the revised manuscript and Lines 317-326 Page 14 to Lines 327-345 Page 15 of the revised manuscript.

Additional comments

Comment 1.

The nomenclature of NSA should be checked and made consistent throughout the manuscript and SI. The SI tables refer to "nitrosulfonic acid," whereas the main manuscript uses "nitric sulfuric acid."

Response: Thank you for this valuable suggestion. We sincerely apologize for the inconsistency in the nomenclature of NSA. To ensure consistency throughout the manuscript and Supporting Information (SI), we have replaced "nitrosulfonic acid" with "nitric sulfuric acid" in all relevant sections and tables.

Comment 2.

The authors should carefully check all cluster formulas and notation in the figures and captions, including inconsistent use of "NSA-SA-A," "SA-A-NS," and the definitions of acid/base labels.

Response: Thank you for this valuable suggestion. We have thoroughly checked all cluster formulas, abbreviations, and notations in the main manuscript, Supporting Information, figures, and figure captions. We have corrected the inconsistent use of "NSA-SA-A," "SA-A-NSA," and related cluster notations and have standardized the nomenclature according to the definitions SA = H_2SO_4, A = NH_3, and NSA = O_2NOSO_3H. All occurrences of "NSA-SA-A" in the manuscript have been changed to "SA-A-NSA" to ensure consistent notation throughout the text. We have also carefully checked the molecular formulas and labels of all clusters to ensure consistency between the text, figures, captions, and SI tables.

Comment 3.

The role of hydration and competing bases such as amines should at least be discussed as limitations when the results are extrapolated to heavily polluted urban NPF. The present ACDC system represents an unhydrated SA-NH_3-NSA network and should not be interpreted as a complete description of urban nucleation chemistry.

Response: Thank you for this valuable suggestion. We agree that hydration and competing bases, particularly atmospheric amines, may affect the formation and stability of NSA-containing clusters and should therefore be considered when interpreting the present results under heavily polluted urban conditions. The current ACDC simulations focus on the unhydrated SA-NH_3-NSA system and are intended to isolate the potential role of NSA in sulfuric acid-ammonia nucleation. Therefore, the present results should not be regarded as a complete representation of the complex chemical processes governing urban NPF.

Following the reviewer's suggestion, we have clarified this limitation in the revised manuscript and have avoided overextending the present results to the full complexity of urban atmospheric nucleation. The effects of hydration and competing bases, particularly amines, will be systematically investigated in our future work to further assess the role of NSA under more atmospherically realistic conditions. Based on this, the sentence of "Nevertheless, the present simulations consider an unhydrated SA-A-NSA system and do not account for the effects of

hydration or competing bases such as atmospheric amines, which will be systematically investigated in future studies." has been added in Lines 441-443 Page 19 of the revised manuscript.